

4-2009

Glycerol monolaurate prevents mucosal SIV transmission

Qingsheng Li

University of Minnesota, qli4@unl.edu

Jacob D. Estes

National Cancer Institute, estesj@mail.nih.gov

Patrick M. Schlievert

University of Minnesota, patrick-schlievert@uiowa.edu

Lijie Duan

University of Minnesota

Amanda J. Brosnahan

University of Minnesota

See next page for additional authors

Follow this and additional works at: <https://digitalcommons.unl.edu/biosciqingshengli>

Li, Qingsheng; Estes, Jacob D.; Schlievert, Patrick M.; Duan, Lijie; Brosnahan, Amanda J.; Southern, Peter J.; Reilly, Cavan S.; Peterson, Marnie L.; Schultz-Darken, Nancy; Brunner, Kevin G.; Nephew, Karla R.; Pambuccian, Stefan; Lifson, Jeffrey D.; Carlis, John V.; and Haase, Ashley T., "Glycerol monolaurate prevents mucosal SIV transmission" (2009). *Qingsheng Li Publications*. 12. <https://digitalcommons.unl.edu/biosciqingshengli/12>

This Article is brought to you for free and open access by the Papers in the Biological Sciences at DigitalCommons@University of Nebraska - Lincoln. It has been accepted for inclusion in Qingsheng Li Publications by an authorized administrator of DigitalCommons@University of Nebraska - Lincoln.

Authors

Qingsheng Li, Jacob D. Estes, Patrick M. Schlievert, Lijie Duan, Amanda J. Brosnahan, Peter J. Southern, Cavan S. Reilly, Marnie L. Peterson, Nancy Schultz-Darken, Kevin G. Brunner, Karla R. Nephew, Stefan Pambuccian, Jeffrey D. Lifson, John V. Carlis, and Ashley T. Haase

LETTERS

Glycerol monolaurate prevents mucosal SIV transmission

Qingsheng Li¹, Jacob D. Estes², Patrick M. Schlievert¹, Lijie Duan¹, Amanda J. Brosnahan¹, Peter J. Southern¹, Cavan S. Reilly³, Marnie L. Peterson⁴, Nancy Schultz-Darken⁵, Kevin G. Brunner⁵, Karla R. Nephew⁵, Stefan Pambuccian⁶, Jeffrey D. Lifson², John V. Carlis⁷ & Ashley T. Haase¹

Although there has been great progress in treating human immunodeficiency virus 1 (HIV-1) infection¹, preventing transmission has thus far proven an elusive goal. Indeed, recent trials of a candidate vaccine and microbicide have been disappointing, both for want of efficacy and concerns about increased rates of transmission^{2–4}. Nonetheless, studies of vaginal transmission in the simian immunodeficiency virus (SIV)–rhesus macaque (*Macacca mulatta*) model point to opportunities at the earliest stages of infection in which a vaccine or microbicide might be protective, by limiting the expansion of infected founder populations at the portal of entry^{5,6}. Here we show in this SIV–macaque model, that an outside-in endocervical mucosal signalling system, involving MIP-3 α (also known as CCL20), plasmacytoid dendritic cells and CCR5⁺ cell-attracting chemokines produced by these cells, in combination with the innate immune and inflammatory responses to infection in both cervix and vagina, recruits CD4⁺ T cells to fuel this obligate expansion. We then show that glycerol monolaurate—a widely used antimicrobial compound⁷ with inhibitory activity against the production of MIP-3 α and other proinflammatory cytokines⁸—can inhibit mucosal signalling and the innate and inflammatory response to HIV-1 and SIV *in vitro*, and *in vivo* it can protect rhesus macaques from acute infection despite repeated intra-vaginal exposure to high doses of SIV. This new approach, plausibly linked to interfering with innate host responses that recruit the target cells necessary to establish systemic infection, opens a promising new avenue for the development of effective interventions to block HIV-1 mucosal transmission.

To understand how SIV infection in a small founder population of cells at the portal of entry transitions in less than two weeks to systemic infection, with massive levels of viral replication and depletion of gut CD4⁺ T cells^{5,6,9,10}, we analysed the anatomical and temporal expansion of these small founder cell populations. We created atlases of the numbers and locations of SIV RNA⁺ cells detected by *in situ* hybridization in cervical and vaginal tissues from animals at 4–10 days post-inoculation (d.p.i.), with the rationale that by locating sites that initially had the largest numbers of infected cells, and then determining how infection expanded and spread from these infected founder populations, we would gain insight into the sites of virus entry and subsequent events underlying the expansion on which systemic infection depends.

In screening 20–40 sections of cervical and vaginal tissues from each animal in this 4–10 d.p.i. time frame, we identified sections with

SIV RNA⁺ cells in nine animals, and in each animal we found one predominant focus of infected cells in the endocervix. There were further clusters of infected cells in the transformation zone (the junction of ecto- and endocervix) adjoining the endocervical and vaginal foci in three animals. We illustrate at the bottom of Fig. 1a the thumbnail representative images of the montages created from the captured images of sections from these animals, and in Fig. 1b a small cluster of SIV RNA⁺ cells found at 4 d.p.i. only in endocervix, and then in 1 out of 40 sections in one isolated area, as reported previously⁶. We mapped onto a two-dimensional grid the positions of cell centres (centroids) of SIV RNA⁺ cells in this focus (Fig. 1c), and predominant foci at 6–10 d.p.i. that were again found in endocervix.

These atlases showed that infection expands by accretion of new infections around an initial cluster of infected cells in endocervix, rather than by diffuse spread of infection in the submucosa, and that the successive influxes of new CD4⁺ T target cells in inflammatory infiltrates fuel local expansion. The marked growth of SIV RNA⁺ clusters is evident from comparisons of the map dimensions from 4 to 10 d.p.i. (Fig. 1d, e and Supplementary Fig. 1a–c), and from the growth of clusters amid inflammatory cell infiltrates at 6 d.p.i. (Fig. 1f), in which SIV RNA⁺ cells are located among dark staining nuclei of cells in inflammatory infiltrates. These focal infiltrates contained increased numbers of CD4⁺ T cells compared to uninfected animals or at 1 d.p.i., and were apparent at 4 d.p.i. (Fig. 2a–c and Supplementary Fig. 2). Virtually all of the infected cells were CD3⁺ CD4⁺ T cells (Fig. 2d).

The isolated focus at 4 d.p.i. seemed unlikely by itself to have induced such an extensive influx of CD4⁺ T cells, and indeed we found evidence implicating endocervical epithelium and plasmacytoid dendritic cells (pDCs) in the initial recruitment of target cells to the endocervical submucosa. We had previously stained these tissues for a pDC marker¹¹, CD123 (also known as IL3RA), to investigate the possible role of pDCs in a ‘premature’ T-regulatory response to infection¹², and now noted areas with CD123⁺ pDCs aligned just beneath the endocervical epithelium. These subepithelial pDC collections were observed at 1 d.p.i., and were not seen in the same numbers or location in uninfected animals (Fig. 3a–c). The pDCs also stained positive for the specific marker BDCA2 (also known as CLEC4C)¹¹ (data not shown), were strongly positive for interferons α (Fig. 3d) and β (data not shown), and expressed the CCR5⁺ cell-attracting chemokines MIP-1 α (CCL3) and MIP-1 β (CCL4) (Fig. 3e), which could thus serve as one mechanism to quickly recruit CD4⁺ T

¹Department of Microbiology, Medical School, University of Minnesota, MMC 196, 420 Delaware Street S.E., Minneapolis, Minnesota 55455, USA. ²AIDS and Cancer Virus Program, Science Applications International Corporation–Frederick, Inc., National Cancer Institute, Frederick, Maryland 21702, USA. ³Division of Biostatistics, School of Public Health, University of Minnesota, MMC 303, 420 Delaware Street S.E., Minneapolis, Minnesota 55455, USA. ⁴Department of Experimental and Clinical Pharmacology, College of Pharmacy, University of Minnesota, 2001 Sixth Street S.E., Minneapolis, Minnesota 55455, USA. ⁵Wisconsin National Primate Research Center, University of Wisconsin, 1220 Capitol Court, Madison, Wisconsin 53715, USA. ⁶Department of Laboratory Medicine and Pathology, Medical School, University of Minnesota, MMC 76, 420 Delaware Street S.E., Minneapolis, Minnesota 55455, USA. ⁷Department of Computer Science and Engineering, Institute of Technology, University of Minnesota, 200 Union Street S.E., Minneapolis, Minnesota 55455, USA.

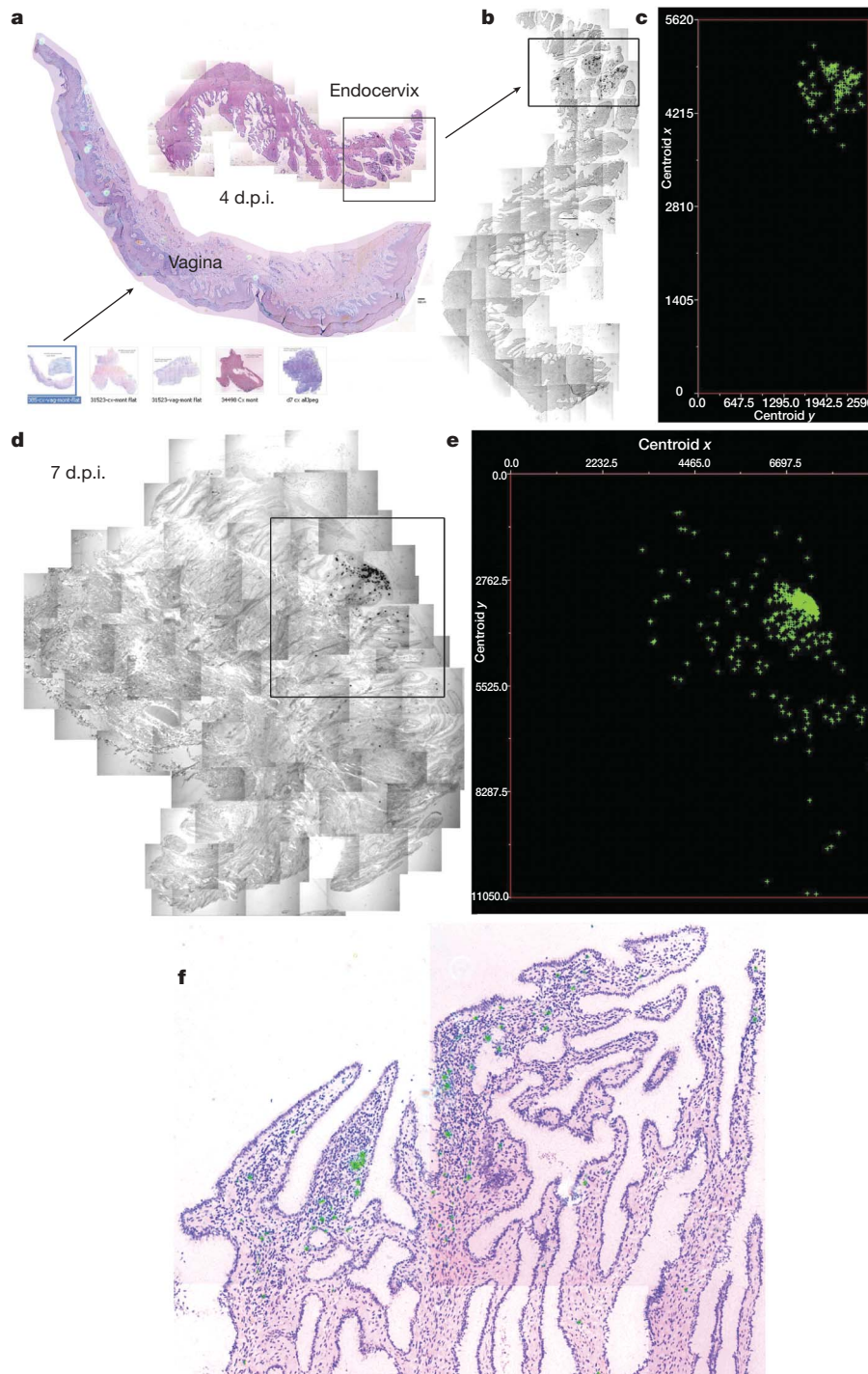


Figure 1 | Mapping early expansion of infection in endocervix. SIV RNA⁺ cells appear black in transmitted light, green in reflected light and in maps. **a–c**, The arrow from the thumbnail montage images (bottom of **a**) of cervix and vagina (4–10 d.p.i.) points to an enlarged image and map of a single focus (box) of SIV RNA⁺ cells in endocervix (4 d.p.i.). Anticlockwise-rotated

image of focus (box) (**b**) and map of *x*, *y* coordinates (μm) (**c**) of cell centroids to the right. **d**, **e**, Endocervical focus (**d**) and map (**e**) (7 d.p.i.) are shown. **f**, Endocervical focus (6 d.p.i.) SIV RNA⁺ cells (green) are concentrated in an inflammatory infiltrate (cells with dark staining nuclei). Original magnification for all images, $\times 10$.

cells to the endocervix. We also found increased expression at 1 and 3 d.p.i. of cervical MIP-3 α , the principal chemokine known to induce pDC migration and T cells into peripheral tissues¹³, in microarray comparisons of uninfected and infected animals (Supplementary Table 1), and increased MIP-3 α staining in endocervical epithelium (Fig. 3f). These findings demonstrate an outside-in signalling pathway triggered by exposure to the viral inoculum that recruits pDCs and T cells to create an environment rich in target cells at the sites of initial infection.

This initial influx of CD4⁺ T cells was followed by a secondary inflammatory process, probably driven by RANTES and other chemokine-producing cells within inflammatory infiltrates (Supplementary Fig. 3), in which SIV RNA⁺ cells were clearly concentrated at 10 d.p.i. (Supplementary Fig. 1d). Unlike endocervix, we saw no evidence for a signalling pathway capable of recruiting additional CD4⁺ T cells in the foci of SIV RNA⁺ cells in the transformation zone and vagina in three animals. However, an inflammatory response provided susceptible target cells for expansion of the infection at these

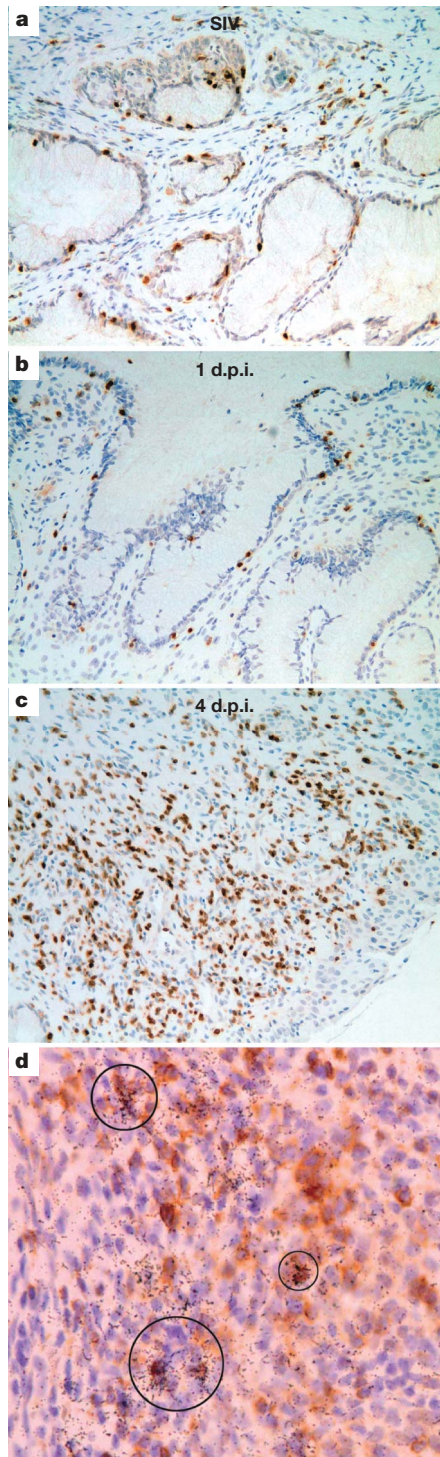


Figure 2 | Influx and infection of CD4⁺ T cells in cervix in early infection. **a–c**, Sections stained with anti-CD4 antibody. Note the relative paucity of CD4⁺ cells in an SIV⁻ (negative animal) (**a**), or an SIV-inoculated animal 1 d.p.i. (**b**), compared to increased numbers of CD4⁺ cells seen in an infected animal at 4 d.p.i. (**c**). **d**, SIV RNA⁺ cells in infiltrates are CD3⁺ T cells. Encircled SIV RNA⁺ cells (overlying black silver grains) are stained brown with anti-CD3. Original magnification, $\times 10$ (**a–c**) and $\times 20$ (**d**).

sites as well, because infected cells (Supplementary Fig. 4a) were generally in areas of inflammation containing IL-8⁺ cells, with associated epithelial thinning and disruption (Supplementary Fig. 4b, c). Thus, inflammation with increases in susceptible target populations is the common denominator across sites.

The importance of the innate immune and inflammatory response in providing new target cells for local expansion and systemic dissemination

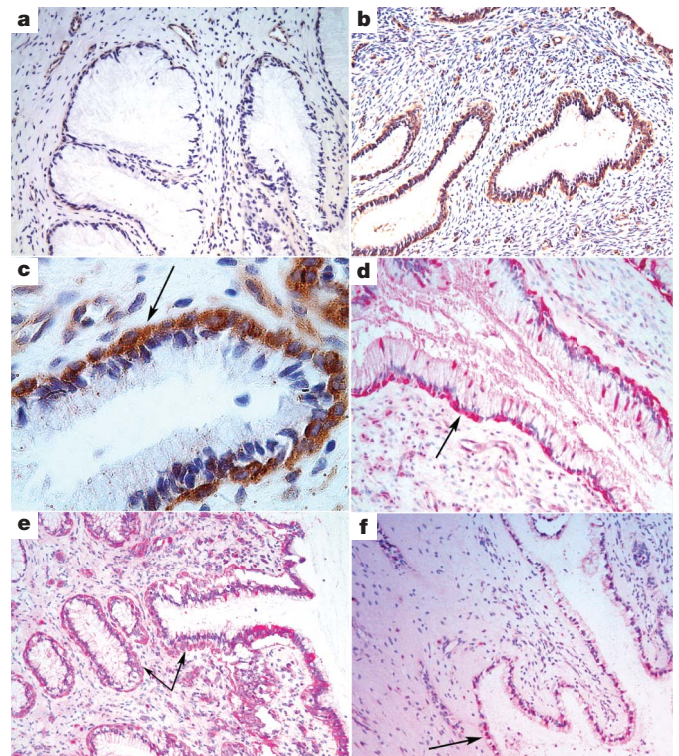


Figure 3 | pDCs, cytokines and chemokines associated with endocervical epithelium after exposure to SIV. **a**, Uninfected animal, original magnification $\times 10$. **b, c**, Rapid accumulation of pDCs beneath endocervical epithelium at 1 d.p.i. shown at $\times 10$ (**b**) and $\times 40$ (**c**) original magnifications. pDCs stained brown with anti-CD123 antibody. Arrow in **c** points to the location of pDCs beneath the epithelium. **d, e**, Arrows point to subepithelial pDCs stained red with anti-interferon- α antibody at 1 d.p.i. (**d**, $\times 20$ magnification) or with anti-MIP-1 β antibody (**e**, $\times 10$ magnification). **f**, Arrow points to MIP-3 α ⁺ endocervical epithelium (red) at 1 d.p.i. Original magnification in **f**, $\times 10$.

suggested that inhibiting this immunoinflammatory process might prevent transmission and systemic infection. We focused on glycerol monolaurate (GML) because of the compound's documented relevant activities in inhibiting immune activation and chemokine and cytokine production by human vaginal epithelial cell cultures (HVECs) on exposure to staphylococcal toxins^{8,14}. We showed that GML inhibited the production of MIP-3 α and IL-8 (as a general marker of inflammation and increased susceptibility to HIV-1 infection in female genital tissues¹⁵) by HVECs in response to the more relevant exposure to HIV-1 (Fig. 4a, b). MIP-3 α and IL-8 levels were also reduced in cervical and vaginal fluids collected in a safety study¹⁶ from rhesus macaques treated intra-vaginally with 5% GML daily for 6 months (Fig. 4c, d).

Encouraged by these results, we tested the potential efficacy of GML against repeated high dose intra-vaginal SIV challenges in ten animals, in an extension of the GML safety study¹⁶. We first evaluated its efficacy in a pilot study in which we could examine cervical and vaginal and lymphatic tissues obtained at the expected peak of viral replication at 14 d.p.i.⁶. Two animals from the safety study that were treated daily with 5% GML in K-Y warming gel, and two animals that received K-Y warming gel alone as a vehicle control, were challenged intra-vaginally 1 h after compound introduction with 10^5 50% tissue-culture infective dose units (TCID₅₀) of SIV. Four hours later they were again given either GML or K-Y warming gel, and challenged after 1 h with an equivalent dose of SIV, and then continued on daily doses of either GML or K-Y warming gel.

Both of the GML-treated animals were completely protected from this high dose SIV challenge. Using *in situ* hybridization there was no evidence for SIV RNA⁺ cells in cervical, vaginal (Supplementary

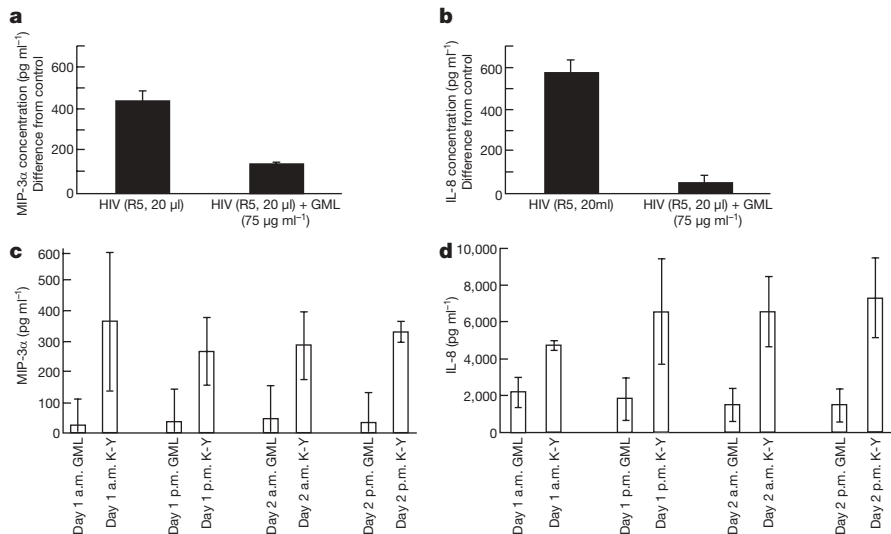


Figure 4 | GML inhibits HIV-1 induced expression of MIP-3 α and IL-8 in HVECs and in cervical and vaginal fluids. **a, b**, R5 isolate of HIV-1 added to HVECs in the amounts indicated \pm GML. MIP-3 α (**a**) and IL-8 (**b**) release from HVECs was measured and expressed as the difference from control. **c, d**, At the end of a 6-month safety study, cervical and vaginal fluids were collected with a swab that reproducibly adsorbed 0.1 ml of fluid from animals that received GML or K-Y warming gel in the a.m. and p.m. of two successive days. MIP-3 α (**c**) and IL-8 (**d**) were measured by ELISA. Bars indicate s.e.m.

Fig. 5a, b) or lymphatic tissues (data not shown), and no evidence of inflammation (Supplementary Fig. 5a, b) or virus detectable in plasma (Fig. 5a). In contrast, in one of the two controls, SIV RNA⁺ cells were detected in endocervical, vaginal (Supplementary Fig. 5c, d) and lymphatic tissues (data not shown) and there was an influx of inflammatory cells associated with infection in the endocervix and vagina (Supplementary Fig. 5c, d), and high levels of virus in plasma (Fig. 5a) were all readily apparent. We then challenged three other GML-treated animals and three K-Y warming gel controls, repeating the challenges 4 weeks later if the animals showed no evidence of systemic infection (plasma levels of <20 copies of SIV RNA per ml). Again, GML prevented acute systemic infection after four exposures to this high dose vaginal challenge, whereas all three control animals became infected (Fig. 5b).

In seeking interventions to prevent vaginal transmission in a SIV-macaque model, we have focused on the critical window of opportunity at the earliest stages of infection when infected founder cell populations are small, and the virus must overcome the limited availability of susceptible target cells to sustain and sufficiently expand the initially infected founder cell populations to disseminate and establish a self-propagating infection in secondary lymphoid organs⁵. Here we show that SIV exploits the innate immune and inflammatory response to overcome this inherent limitation in the availability of target cells in the endocervix—the predominant site of the initial infected cell clusters. We document the growth of clusters by accretion of new infections in influxes of CD4⁺ T cell targets, and provide evidence plausibly linking the first influx to an outside-in mucosal signalling pathway in which the exposure of endocervical epithelium to the viral inoculum increases the expression of MIP3- α to recruit pDCs, which in turn produce MIP-1 α and MIP-1 β to recruit CCR5⁺ targets.

The discovery reported here of *in vivo* induction of MIP3- α in endocervical epithelium, together with our *in vitro* results and the previous report of the induction of MIP3- α in uterine epithelial cultures by microbial-related stimuli¹⁷, point to outside-in signalling as a general feature of mucosal epithelium of the upper female genital tract. This signalling pathway and the production of interferons and virus-inhibiting chemokines by pDCs, support the concept that the mucosal lining of the upper female genital tract is truly the front line of the innate mucosal immune system¹⁸. Although our conclusion that innate defences there are actually critical to the establishment and spread of infection may thus at first seem counterintuitive, it is in keeping with the previous report of possibly enhanced vaginal transmission with agonists used to stimulate innate immunity¹⁹, and with the concept advanced here: although interferons and anti-viral chemokines produced locally by pDCs may protect themselves and

contribute to limiting infection initially, on balance, SIV's greater immediate need is for target cells, which is served by the inflammatory component of the innate immune response.

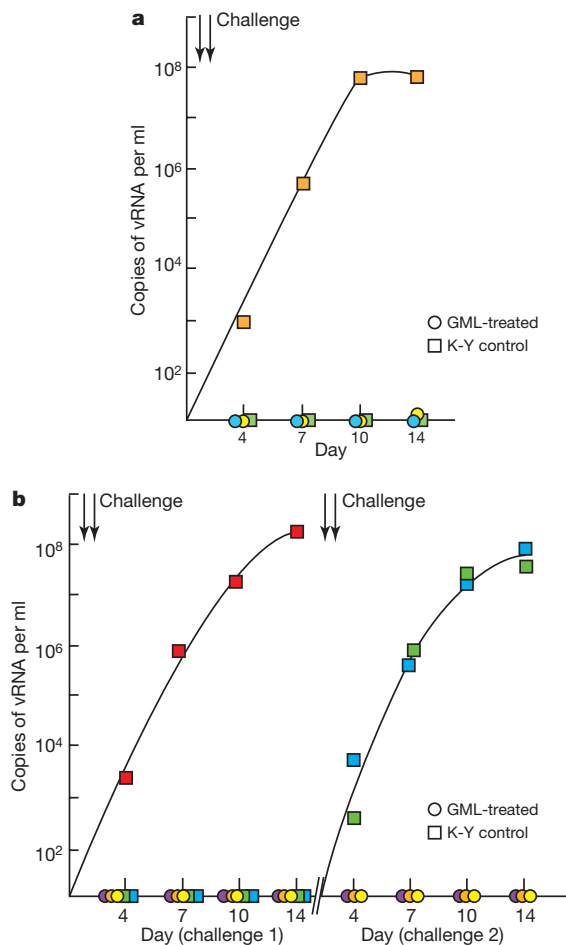


Figure 5 | GML prevents mucosal transmission and acute infection. **a**, Pilot experiment continuation of daily dosing safety study. Two animals treated with GML in K-Y warming gel (circles) and two treated with gel only (squares) were challenged twice (two arrows), 1 h after treatment, with 10⁵ TCID₅₀ of SIV. Colours indicate individual animals. SIV RNA in plasma was measured to peak viremia, 14 d.p.i. **b**, Three animals treated with GML and three given K-Y warming gel were challenged as described in **a**. The animals that were not infected were treated and challenged again 4 weeks later, shown at the right.

We show that GML can break this vicious cycle of signalling and inflammatory responses in the cervix and vagina to prevent acute SIV infection in five out of five animals with repeated intra-vaginal challenges of 10^5 TCID₅₀ of SIV, and particularly notably, in three out of three animals challenged four times with this high dose. This result represents a highly encouraging new lead in the search for an effective microbicide to prevent HIV-1 transmission that meets the criteria of safety, affordability and efficacy²⁰. GML is a US Federal Drug Administration (FDA) generally recognized as safe (GRAS)⁷ agent that has been applied daily intra-vaginally in K-Y warming gel, an FDA-approved vehicle for human vaginal use, for 6 months in rhesus macaques with no evidence of pathological effects or alteration of resident *Lactobacilli*¹⁶. GML is inexpensive (each dose used here cost less than 1 cent), and is efficacious in preventing acute systemic infection. Certainly, longer-term and well-powered studies with larger numbers of animals will be needed to definitively establish efficacy, and efficacy against occult infections, reportedly manifest as long as a year after repeated low-dose intravaginal inoculations²¹, and for which we now have preliminary evidence in this repeated high-dose model in one of the three animals with previously undetectable virus. Even conservative estimates of efficacy $\geq 60\%$ (see Methods) extrapolate, according to mathematical models, to 2.5 million averted HIV infections over a 3-year period²², thus providing rationale and motivation for human trials of GML alone as a microbicide, and/or combined with other agents that specifically inhibit HIV-1 replication²³. More generally, other microbes may exploit mucosal signalling and the innate inflammatory response to establish infection, so that GML may be the first example of a class of compounds that provide protection by interfering with these responses.

METHODS SUMMARY

Animals, inoculation of SIV, GML and K-Y warming gel. Adult female rhesus macaque monkeys (*Macaca mulatta*), housed in accordance with the regulations of the American Association of Accreditation of Laboratory Animal Care standards, were inoculated twice intra-vaginally with 1 ml of 10^5 TCID₅₀ per ml SIVmac 251 (ref. 6). One-ml of K-Y warming gel $\pm 5\%$ GML was administered atraumatically into the vagina daily and before viral challenges.

SIV RNA in plasma. SIV RNA copy equivalents per ml (Eq ml⁻¹) in plasma was determined using a quantitative PCR with reverse transcription (qRT-PCR) assay²⁴.

In situ hybridization and immunohistochemistry. Blood, cervical, vaginal and lymphoid tissues were collected from euthanized animals, fixed and then embedded in paraffin. *In situ* hybridization combined with immunohistochemical staining and immunochemistry were performed as described^{9,12}.

Digital atlases. Images of fields with SIV RNA⁺ cells were acquired, merged (Photoshop 7.0 automerger), and, after using Photoshop Action procedures to delineate SIV RNA⁺ cells, centroid *x*, *y* coordinates were assigned using MetaMorph software, and the coordinates were plotted with Excel.

Induction and measurement of MIP-3 α and IL-8. HIV-1 \pm GML was added to HVECs cultured as described²⁵. Chemokines in the supernatants were measured by ELISA²⁵.

Microarray analysis. Gene expression profiles in cervix before and after intra-vaginal SIV inoculation were analysed with the Affymetrix GeneChip Rhesus Macaque Genome Array as described²⁶.

Statistical methods. The negative binomial distribution was used to model repeated challenges. The model assumes that outcomes for distinct animals are independent, and that the probability of being infected differs between the two groups. The use of maximum likelihood or Bayesian methods (which don't assume the sample size is large) both indicate that the efficacy of GML against transmission is at least 65%, in which the posterior probability that GML is more likely to prevent infection than K-Y warming gel is 0.98, and the *P*-value that the probability differs between groups is 0.04.

Full Methods and any associated references are available in the online version of the paper at www.nature.com/nature.

Received 20 November 2008; accepted 20 January 2009.

Published online 4 March 2009.

1. Fauci, A. S. 25 years of HIV. *Nature* **453**, 289–290 (2008).
2. Ledford, H. HIV vaccine may raise risk. *Nature* **450**, 325 (2007).
3. Check, E. Scientists rethink approach to HIV gels. *Nature* **446**, 12 (2007).

4. Cohen, J. AIDS research. Microbicide fails to protect against HIV. *Science* **319**, 1026–1027 (2008).
5. Haase, A. T. Perils at mucosal front lines for HIV and SIV and their hosts. *Nature Rev. Immunol.* **5**, 783–792 (2005).
6. Miller, C. J. et al. Propagation and dissemination of infection after vaginal transmission of SIV. *J. Virol.* **79**, 9217–9227 (2005).
7. Kabara, J. J. in *Cosmetic and Drug Preservation* (eds Kabara, J. J. et al.) 305–322 (Marcel Dekker, Inc, 1984).
8. Peterson, M. L. & Schlievert, P. M. Glycerol monolaurate inhibits the effects of Gram-positive select agents on eukaryotic cells. *Biochemistry* **45**, 2387–2397 (2006).
9. Li, Q. et al. Peak SIV replication in resting memory CD4⁺ T cells depletes gut lamina propria CD4⁺ T cells. *Nature* **434**, 1148–1152 (2005).
10. Mattapallil, J. J. et al. Massive infection and loss of memory CD4⁺ T cells in multiple tissues during acute SIV infection. *Nature* **434**, 1093–1097 (2005).
11. Colonna, M., Trinchieri, G. & Liu, Y. J. Plasmacytoid dendritic cells in immunity. *Nature Immunol.* **5**, 1219–1226 (2004).
12. Estes, J. D. et al. Premature induction of an immunosuppressive regulatory T cell response during acute simian immunodeficiency virus infection. *J. Infect. Dis.* **193**, 703–712 (2006).
13. Dieu-Nosjean, M. C., Vicari, A., Lebecque, S. & Caux, C. Regulation of dendritic cell trafficking: a process that involves the participation of selective chemokines. *J. Leukoc. Biol.* **66**, 252–262 (1999).
14. Schlievert, P. M., Deringer, J. R., Kim, M. H., Projan, S. J. & Novick, R. P. Effect of glycerol monolaurate on bacterial growth and toxin production. *Antimicrob. Agents Chemother.* **36**, 626–632 (1992).
15. Narimatsu, R., Wolday, D. & Patterson, B. K. IL-8 increases transmission of HIV type 1 in cervical explant tissue. *AIDS Res. Hum. Retroviruses* **21**, 228–233 (2005).
16. Schlievert, P. M. et al. Glycerol monolaurate does not alter rhesus macaque (*Macaca mulatta*) vaginal lactobacilli and is safe for chronic use. *Antimicrob. Agents Chemother.* **52**, 4448–4454 (2008).
17. Crane-Godreau, M. A. & Wira, C. R. CCL20/macrophage inflammatory protein 3 α and tumor necrosis factor α production by primary uterine epithelial cells in response to treatment with lipopolysaccharide or Pam3Cys. *Infect. Immun.* **73**, 476–484 (2005).
18. Wira, C. R., Fahey, J. V., Sentman, C. L., Pioli, P. A. & Shen, L. Innate and adaptive immunity in female genital tract: cellular responses and interactions. *Immunol. Rev.* **206**, 306–335 (2005).
19. Wang, Y. et al. The Toll-like receptor 7 (TLR7) agonist, imiquimod, and the TLR9 agonist, CpG ODN, induce antiviral cytokines and chemokines but do not prevent vaginal transmission of simian immunodeficiency virus when applied intravaginally to rhesus macaques. *J. Virol.* **79**, 14355–14370 (2005).
20. Klasse, P. J., Shattock, R. J. & Moore, J. P. Which topical microbicides for blocking HIV-1 transmission will work in the real world? *PLoS Med.* **3**, e351 (2006).
21. Ma, Z.-M., Abel, K., Rourke, T., Wang, Y. & Miller, C. J. A period of transient viremia and occult infection precedes persistent viremia and antiviral immune responses during multiple low-dose intravaginal simian immunodeficiency virus inoculations. *J. Virol.* **78**, 14048–14052 (2004).
22. Johnston, R. Microbicides 2002: an update. *AIDS Patient Care STDS* **16**, 419–430 (2002).
23. Shattock, R. J. & Moore, J. P. Inhibiting sexual transmission of HIV-1 infection. *Nature Rev. Microbiol.* **1**, 25–34 (2003).
24. Cline, A. N., Bess, J. W., Piatak, M. Jr & Lifson, J. D. Highly sensitive SIV plasma viral load assay: practical considerations, realistic performance expectations, and application to reverse engineering of vaccines for AIDS. *J. Med. Primatol.* **34**, 303–312 (2005).
25. Peterson, M. L. et al. The innate immune system is activated by stimulation of vaginal epithelial cells with *Staphylococcus aureus* and toxic shock syndrome toxin 1. *Infect. Immun.* **73**, 2164–2174 (2005).
26. Li, Q. et al. Functional genomic analysis of the response of HIV-1 infected lymphatic tissue to antiretroviral therapy. *J. Infect. Dis.* **189**, 572–582 (2004).

Supplementary Information is linked to the online version of the paper at www.nature.com/nature.

Acknowledgements We thank C. Miller and D. Lu at the California National Primate Research Center, for helpful discussion and virus stocks, J. Kernitz at the Wisconsin National Primate Research Center, for discussion and administrative support, and C. O'Neill and T. Leonard for help with the manuscript and figures. This work was supported in part by National Institute of Health (NIH) grants R21 AI071976 and P01 AI066314 (A.T.H.), funds from the National Cancer Institute, NIH, under contracts N01-CO-12400 and HHSN266200400088C (J.D.L.), and grant number P51 RR000167 from the National Center for Research Resources, a component of the NIH, to the Wisconsin National Primate Research Center. This research was conducted in part at a facility constructed with support from Research Facilities Improvement Program grant numbers RR15459-01 and RR020141-01. This publication's contents are solely the responsibility of the authors and do not necessarily represent the official views of the NCRR or NIH.

Author Information Reprints and permissions information is available at www.nature.com/reprints. Correspondence and requests for materials should be addressed to A.T.H. (haase001@umn.edu).

METHODS

Animals. Adult female rhesus macaque monkeys (*Macaca mulatta*) used in the studies were housed at the California and Wisconsin National Primate Centers in accordance with the regulations of the American Association of Accreditation of Laboratory Animal Care and the standards of the Association for Assessment and Accreditation of Laboratory Animal Care International; all protocols and procedures were approved by the relevant Institutional Animal Care and Use Committee. All animals were negative for antibodies to HIV type 2, SIV, type D retrovirus, and simian T-cell lymphotropic virus type 1.

Intra-vaginal inoculation of SIV, GML and K-Y warming gel. Monkeys were inoculated intra-vaginally twice in a single day, with a 4-h interval between inoculations, with 1 ml of a 2004 virus stock from C. Miller of 10^5 TCID₅₀ per ml SIVmac 251. For inoculation, each animal was anesthetized with an intramuscular injection of a combination of ketamine hydrochloride (Parke-Davis) (up to 7 mg per kg) and medetomidine (up to 5 mg per kg). More ketamine when needed was given intravenously (up to 5 mg per kg). The animal was placed in a sternal position with her posterior elevated approximately 60 degrees from horizontal, and a 1-ml syringe without a needle was inserted atraumatically into the vagina to deliver the inoculum. Animals thereafter remained in the sternal position for between 30 and 40 min. For 5% GML and vehicle control gel dosing, as well as the collection of vaginal swabs, animals were transferred to a table-top restraint device to administer either 1 ml of vehicle control K-Y warming gel or 1 ml of gel containing 50 mg solubilized GML using a 1-ml syringe without a needle inserted atraumatically into the vagina, as described above.

GML formulation. GML (monomuls 90-L 12, Cognis Corporation Care Chemicals) was dissolved in K-Y warming gel (5 g per 100 ml) at the Fairview Compounding Pharmacy.

Detection of SIV RNA in plasma. SIV viral RNA (vRNA) genomic copy equivalents in EDTA-anti-coagulated plasma was determined using a qRT-PCR procedure modified from an assay described previously²⁴. In brief, vRNA was isolated from plasma using a GuSCN-based procedure as described. qRT-PCR was performed using the SuperScript III Platinum(R) One-Step Quantitative RT-PCR System (Invitrogen). Reactions were run on a Roche LightCycler 2.0 instrument and software. vRNA copy number was determined using LightCycler 4.0 software (Roche Molecular Diagnostics) to interpolate sample crossing points onto an internal standard curve prepared from tenfold serial dilutions of a synthetic RNA transcript representing a conserved region of SIV gag.

Tissue collection and processing. At the time of euthanasia, blood, upper, middle and lower portions of vagina, cervix and uterus, draining lymph nodes (iliac, obturator and inguinal), mesenteric, axillary and inguinal lymph nodes, and gut (ileum, jejunum and colon) from each animal were collected and fixed in 4% paraformaldehyde, SafeFix II (Fisher Scientific) or Streck's fixative (Streck Laboratories, Inc.), and embedded in paraffin for sectioning.

In situ hybridization. *In situ* hybridization to detect SIV RNA was performed as previously described⁹. In brief, after deparaffinization and pretreatment to permeabilize tissue and block nonspecific binding, 5- μ m sections from 4% paraformaldehyde-fixed tissues were hybridized to ³⁵S-labelled SIV RNA antisense or sense (as a negative control) riboprobes covering more than 90% of SIV genome. After overnight hybridization, the sections were washed, digested with RNases, coated with nuclear track emulsion, exposed, developed and counterstained with haematoxylin and eosin.

Construction of digital atlas of SIV vRNA⁺ cells in cervix and vagina. An image of each field with SIV RNA⁺ cells detected by *in situ* hybridization was collected sequentially using epifluorescent illumination, Olympus B-MAX microscope, and a 'spot insight' digital camera (Diagnostic Instruments). To create the montage image, the images from each section were acquired from left to right and from top to bottom, with a ~20% overlap with the neighbouring images to avoid gaps. Images were automatically merged into one Atlas image using a Photoshop 7.0 automerge function. After using the Photoshop Action procedures to associate individual silver grains with cells, the centroid *x*, *y* coordinates of a SIV RNA⁺ cell were assigned using MetaMorph (version 7.1.3.) software, and these coordinates were then logged into Excel files as numeric numbers and plotted with Excel.

Immunohistochemistry. Immunohistochemistry was performed as described^{9,12} using a biotin-free detection system, MACH-3 (Biocare Medical) or EnVision⁺ System (DakoCytomation), on 5- μ m tissue sections mounted on glass slides. Tissues were deparaffinized and rehydrated in deionized water. Heat-induced epitope retrieval was performed using the water-bath method (95–98 °C for 10–20 min) in one of the following buffers: EDTA Decloaker reagent (Biocare Medical), DiVA Decloaker (Biocare Medical), 10 mM sodium citrate, pH 6.0, or 1 mM EDTA, pH 8.0, followed by cooling to room temperature. Tissues sections were blocked with SNIPER Blocking Reagent (Biocare Medical) for 1 h at room temperature. Endogenous peroxidase was blocked with 3% (v/v) H₂O₂ in TBS

(pH 7.4). Primary antibodies were diluted in 10% SNIPER Blocking Reagent in TNB (Tris-HCl, pH 7.5, 0.15 M NaCl, 0.05% Tween 20 with Dupont blocking buffer) and incubated overnight at 4 °C. After the primary antibody incubation, sections were washed and then incubated with mouse, goat or rabbit polymer system reagents conjugated with either horseradish peroxidase or alkaline phosphatase according to the manufacturer's instructions, and developed with 3,3'-diaminobenzidine (Vector Laboratories) or Vulcan Fast Red (Biocare Medical). Sections were counterstained with CAT Haematoxylin (Biocare Medical), mounted in Permount (Fisher Scientific) and examined by light microscopy. Primary antibodies and other reagents and protocols used are summarized in Supplementary Table 2. All anti-human antibody reagents were demonstrated to show good cross reactivity with the cognate macaque antigens. Isotype-matched IgG negative control antibodies in all instances yielded negative staining results.

Immunohistochemical staining and *in situ* hybridization. Combined immunohistochemical staining and *in situ* hybridization were performed as described previously⁹. In brief, sections were microwaved for antigen retrieval, hybridized, washed and digested with RNases, incubated with antibody markers for cell type, CD3, CD4, CD68, and then stained with the Dako EnVision⁺ Peroxidase kit with antibodies to the primary antibody and diaminobenzidine. After washing, the sections were coated with nuclear track emulsion, exposed, developed and counterstained with haematoxylin.

Culture of HVECs and induction and measurement of MIP-3 α and IL-8. HVECs were cultured until confluent at 37 °C, 7% CO₂ in 96-well flat-bottom microtitre plates (Becton Dickinson Labware) in 100 μ l per well of keratinocyte serum free medium with antibiotics²⁵. HIV-1 \pm GML was added to wells, and, after 6-h incubation, supernatants were collected and tested for chemokines by ELISA as described by the manufacturer (R&D Systems). Data reported are mean \pm s.d. We have previously shown²⁵ that GML does not interfere with ELISA for chemokine detection.

Microarray analysis of cervical transcriptional responses to intravaginal SIV inoculation. Gene expression profiles in cervix of macaques before and after intravaginal SIV inoculation at 1 and 3 d.p.i. were analysed with the GeneChip Rhesus Macaque Genome Array (Affymetrix, Inc.), which contains ~47,000 rhesus transcripts. RNA extractions, preparation of biotin-labelled complementary RNA (cRNA) probes, and microarray hybridization followed previously published protocols²⁶. In brief, snap-frozen cervical tissues from two uninfected and three infected Indian rhesus macaques at 1 d.p.i., and from two macaques at 3 d.p.i. were homogenized, total RNA was extracted, double-stranded complementary DNA and biotin-labelled cRNA probes were synthesized from 5 μ g of total RNA. Fifteen micrograms of fragmented cRNA was hybridized to an Affymetrix GeneChip Rhesus Macaque Genome Array. After hybridization, chips were washed, stained with streptavidin-phycoerythrin, and scanned with GeneChip Operating Software at the Biomedical Genomics Center at the University of Minnesota. The experiments from each RNA sample were duplicated in the preparation of each cRNA probe, and microarray hybridization. Microarray data were analysed in Expressionist program Genedata, Pro version 4.5, using the robust multi-array analysis (RMA) algorithm. The expression levels from duplicated chips of the same animals' RNA were correlated and averaged. Tests for differences between the uninfected and infected animals at 1 and 3 d.p.i. were conducted using the two-sample *t*-test. Cutoff was set at $P < 0.05$ and ≥ 2 -fold increased expression.

Statistical methods. In the initial protocol, animals were challenged twice and then necropsied at peak replication to obtain tissues to evaluate viral replication, whereas in the second experiment, each animal was repeatedly challenged until all of the controls were infected. For this second experiment, we used the negative binomial likelihood as a statistical model to interpret the results of the experiment. Note that because the design of the second stage of the experiment included the possibility that treated animals would never get infected, animals in the treatment group who were uninfected were considered to be right censored at the trial at which all the controls were finally infected. Because the challenge involved two doses at each time point, our trials consist of two such doses. Therefore, an animal that survived two challenges was subjected to four doses. Our model supposes that a success for a trial occurs when an animal is infected by one of these double-dose challenges. Moreover, the model supposes that the outcome for each animal is independent and that there is a different probability of a success for a trial depending on treatment status. Hence, if we let θ represent the probability that an animal is infected with one challenge, and an animal is infected on the *m*th challenge, then this animal contributes a factor of $(1 - \theta)^{m-1} \times \theta$ to the likelihood. For an animal that survives *m* such challenges, because the probability that this occurs is $(1 - \theta)^m$, this animal would contribute $(1 - \theta)^m$ to the likelihood. The likelihood for each group is calculated by multiplying the contributions from each animal in that group. Maximum likelihood estimates are then determined by maximizing the likelihood. We can also compute Bayesian credible sets and the posterior probability that the probability

of success differs between the two groups using numerical integration (using an adaptive 15-point Gauss–Kronrod quadrature, as implemented in the software S-plus, version 3.4 release 1, from Mathsoft, Inc.). For the groups of three animals challenged four times, the efficacy of GML against transmission is estimated to be at least 65%, and the probability that GML is more likely to prevent infection than K-Y warming gel alone is 0.98. Although we prefer this estimate, because the outcome was determined decisively, including the animals in the pilot experiment in which we did not repeatedly challenge until infected, five out of five GML-treated animals, and one out of five controls did not get infected. The estimated efficacy of GML (using the same methods) in this case is at least 72% at a probability of 0.95.